

Article

Chromium and Copper-Doped Magnetite Catalysts for the High Temperature Shift Reaction

Emerentino Brazil Quadro, Maria de Lourdes Ribeiro Dias, Adelaide Maria Mendonça Amorim, and Maria do Carmo Rangel

Instituto de Química, Universidade Federal da Bahia, 40170-280 Salvador - Ba, Brazil

Foi obtida magnetita pura e dopada com cromo e cobre, visando produzir catalisadores, na fase ativa, destinados à conversão de monóxido de carbono a dióxido de carbono a altas temperaturas (reação de HTS). As amostras foram preparadas por aquecimento do hidróxido de ferro (III), IHA, na faixa de 150-400 °C, e caracterizados por análise química, difração de raios-X, análise térmica (DSC e TG), espectroscopia no infravermelho, medidas de área específica, microscopia eletrônica de varredura e microsonda eletrônica de raios X. Observou-se que a presença do cobre favorece a formação da magnetita mas não afeta a cristalinidade dos sólidos, de modo significativo. Ambos os dopantes melhoram o desempenho dos catalisadores: o cromo atua como estabilizador, enquanto o cobre aumenta a atividade intrínseca. Entretanto, este último favorece a sinterização, levando à formação de sólidos com baixas áreas superficiais. O efeito sinérgico desses dopantes é aumentar a atividade catalítica e a área superficial dos sólidos.

Copper and chromium-doped magnetite was prepared to be used as catalysts, in the active phase, in the high temperature shift (HTS) reaction. Samples were produced by heating a mixed hydrate ferric oxyhydroxide (IHA) in the range of 150-400 °C and characterized by means of chemical analysis, X-ray diffraction, thermal analysis (DSC and TG), infrared spectroscopy, surface area measurements, scanning electron microscopy and X-ray microanalysis. It was found that copper favors magnetite formation but does not affect significantly the crystallinity of the solids. Both chromium and copper improve the performance of the catalysts towards the HTS reaction: chromium acts as a stabilizer whereas copper increases the intrinsic activity. However, copper favors sinterization leading to solids with low surface areas. The increase in the catalytic activity and in the surface area of the solids reflects the synergy of these dopants.

Keywords: *magnetite formation, chromium and copper-doped magnetite, HTS catalyst*

Introduction

The water gas shift reaction¹:



$$\Delta H = -40,6 \text{ kJ mol}^{-1}.$$

is an important step in industrial processes to produce highly pure hydrogen. It is favored by low temperatures and excess of steam due to its reversibility and exothermicity, but it takes high temperatures to achieve suitable rates for commercial applications. As a consequence, this reaction is often carried out in two steps, the first being performed in the range of 320-450 °C (named high temperature shift, HTS) whereas, in the other, carbon monoxide is removed in thermodynamically favorable conditions, at 200-250 °C (low temperature shift, LTS)².

The HTS stage is carried out over three catalytic fixed beds of chromia-doped iron oxides, commercialized as hematite ($\alpha\text{-Fe}_2\text{O}_3$). This compound is reduced in situ to produce magnetite (Fe_3O_4) which is found to be the active phase¹⁻³. This reaction is highly exothermic and should be controlled to avoid the production of metallic iron, which may catalyze undesirable reactions such as hydrocarbon generation². In industrial processes, large amounts of steam are used to inhibit the metallic iron formation. However, this implies high operational costs which lead to the need for developing the catalyst in the active phase.

The chromium and iron-based catalysts have been used in commercial processes for more than sixty years and show high stability and performance. In recent times, these solids have been improved by adding small amounts of copper, resulting in more active and selective catalysts. They have

already been used in industrial plants and are able to work in more severe conditions, *e.g.* lower steam to carbon ratios without being reduced to metallic iron. Therefore, these systems offer greater operating flexibility as compared to the classic HTS catalysts; the highest activity allows the use of smaller bed volume without affecting the plant performance; the protection against metallic iron formation, and hence hydrocarbon production, saves hydrogen and requires lower operating temperatures reducing catalyst sintering rates to ensure long life.

The chromium and iron- based catalysts have been extensively studied. A lot of work has been carried out concerning their activity, selectivity and mechanical strength as well as their resistance against sulphur⁴⁻⁶. The role of chromium was also considered; it is believed to increase the surface area of the solids preventing sintering and thus increasing their life¹⁻³.

On the other hand, there are few works in the open literature about the copper and chromium-doped iron oxides, as HTS catalysts, despite their commercial importance^{7,8}.

Considering these aspects, this work describes a method of preparation to produce this catalyst in the active form, in order to avoid the reduction step before the HTS reaction; this procedure offers the possibility of increasing the life of the catalyst as well as the process efficiency due to the energy saved.

In a previous work⁹, we found that heating of chromium-doped iron (III) hydroxoacetate (IHA) is a convenient method to prepare chromium-doped magnetite, useful as catalysts for the HTS reaction. In the present paper, we continued these studies by using this method to produce the copper and chromium-doped magnetite.

Experimental

All reagents used were of an analytical grade.

Samples were prepared by heating IHA, a hydrate ferric oxyhydroxide, amorphous to X-ray¹⁰, doped with copper, chromium or both, in the range of 150 – 400 °C. The magnetite formation was followed by determining the amount of Fe (II) in solids as well as by X-ray diffraction and by thermal analysis (DSC and TG). Infrared spectroscopy, surface area measurements, scanning electron microscopy and X-ray microanalysis were also used to characterize the materials produced.

The IHA precursors were prepared by reverse coprecipitation techniques at room temperature, followed by heating under nitrogen (100 mL/min) in the range of 150-400 °C, for two hours. Different Fe/Cu molar ratios were used (Fe/Cu = 55 and 35) whereas the amount of chromium in solids was kept the same in all cases, in a value close to those of the commercial formulations (Fe/Cr = 10). Plain IHA was also prepared to be used as a reference.

The copper-doped samples (Fe/Cu = 55) were produced by adding 250 mL of an aqueous solution with 1.079 g of $\text{Cu}(\text{NO}_3)_2 \cdot 3\text{H}_2\text{O}$ and another with 101.0 g of $\text{Fe}(\text{NO}_3)_3 \cdot 9\text{H}_2\text{O}$ to 150 mL of 6 N sodium hydroxide solution under stirring. The final pH was adjusted to 11 and the system was kept under stirring for 30 min. The sol produced was centrifuged (2000 rpm, 5 min) and the gel rinsed with water at 60 °C, to remove sodium and nitrate ions from the starting materials. The supernatant was analyzed for nitrate ions and the gel was washed and centrifuged again. After this, it was rinsed with 100 mL of 5% (w/v) ammonium acetate solution in order to promote acetate sorption on iron (III) hydroxide^{9,10} and the resultant material was dried in an oven at 120 °C. The same procedure was followed to prepare samples with Fe/Cu = 35, by using an amount of 1.7427 g of copper nitrate.

In the preparation of chromium-doped samples, 10.1 g of $\text{Cr}(\text{NO}_3)_3 \cdot 9\text{H}_2\text{O}$ was used instead of copper nitrate in the method described above.

The chromium and copper-doped solids were produced by adding the three solutions simultaneously, in the method described above. The same method was also used to prepare the plain samples.

The qualitative analysis of nitrate was performed by adding about 1 mL of concentrated sulfuric acid to 10 mL of supernatant after centrifugation. The $[\text{Fe}(\text{NO})]^{2+}$ formation was detected by a brown ring¹¹. The absence of nitrate in the solids was confirmed by infrared spectroscopy. To determine the iron content, the solids were dissolved in concentrated hydrochloric acid, under reflux for 10 min. After reducing Fe(III) to Fe(II) with stannous chloride, the solution was titrated with potassium dichromate. The analysis of Fe (II) content was carried out on fresh and on used catalysts to follow the magnetite formation from IHA and its stability under the reaction atmosphere, respectively. The samples were dissolved in concentrated hydrochloric acid, under a carbon dioxide atmosphere and then titrated with potassium dichromate¹². The amount of chromium in the solids was determined by adding ammonium iron (II) sulfate to fused samples to reduce Cr(VI) to Cr(III), followed by back titration of excess of Fe(II) with potassium dichromate¹³. The copper and sodium contents were analyzed by atomic absorption in a Perkin Elmer 703 equipment. Carbon analysis was carried out using a model LECO 761-100 apparatus.

Infrared spectra in the range of 4000-650 cm^{-1} were taken in a Shimadzu IR-430 spectrometer from KI discs. X-ray diffractograms were recorded at room temperature with a Philips PW 1130 instrument using $\text{Cu K}\alpha$ radiation, at a rate of 2 degrees/min. The surface areas were measured in a CG 2000 apparatus (BET method).

Magnetite formation was monitored by carrying out thermal analysis experiments (DSC and TG) at a heating

rate of 10 °C/min, under nitrogen atmosphere (100 mL/min) using a Du Pont 9900 instrument.

X-ray microanalysis were performed in a microprobe Noran attached to a Jeol JSM-T300 microscope operating at 20-30KV.

In order to evaluate the performance of the catalysts, 0.2 cm³ of powder within -250 and +325 mesh size was used in a fixed bed microreactor consisting of a stainless tube. All experiments were carried out under isothermal conditions (370 °C) and at atmospheric pressure, providing there is no diffusion effect. A gas composition around 8.1% CO, 5.3 % CO₂, 47.8% H₂ 38.4 N₂ and 0.2% CH₄ and a steam/gas = 0.6 were employed. The gaseous effluent was analyzed by on line gas chromatography, using a CG-35 instrument, with a thermal conductivity detector (at 100 °C) and a 13X sieve molecular column (2 m, 1/8"), at 40 °C, using hydrogen as carrier (30 mL/min). The reaction was followed by monitoring the carbon monoxide concentration in the stream. A commercial catalyst, based on iron, chromium and copper (87% Fe₂O₃, 10% Cr₂O₃, 3% CuO) was used to compare the performance of the solids prepared. After each experiment, the Fe(II)/Fe(III) ratio was measured to follow the iron reduction under the reaction atmosphere.

Results

Table 1 shows the results of iron, carbon, chromium, sodium and copper analysis. We can see that in copper-doped samples, the experimental Fe/Cu relation is close to the initial ratio when the sample has a low amount of copper. However, in the presence of chromium the reverse behavior is noted. On the other hand, the Fe/Cr ratios are smaller than the values of the starting solutions (10) indicating a high level of precipitation of the chromium compounds as compared to the iron ones.

As ammonia can be complexed by copper in aqueous medium, yielding a blue and soluble compound¹⁴, [Cu(NH₃)₄]²⁺, sodium hydroxide was used instead of ammonium hydroxide to precipitate the mixed IHA. As shown in Table 1, the residual amount of sodium from the precipitate depends on the presence of the dopants as well as on

Table 1. Fe/Na, Fe/Cr, Fe/Cu and Fe/acetate molar ratio for plain and doped IHA.

Sample	Fe/Na (± 0.2)	Fe/Cr (± 0.2)	Fe/Cu (± 0.2)	Fe/Acetate (± 0.2)
IHA	10.4	-	-	5.4
Cr	6.3	5.3	-	7.0
Cu55	7.1	-	54.0	4.2
Cu35	6.2	-	30.2	4.4
CrCu55	6.0	4.7	45.6	5.6
CrCu35	5.1	3.9	38.9	6.5

their contents; the largest amount was detected in the plain sample. The acetate sorption also changes due to the dopant as it can be inferred by the iron to acetate molar ratios.

The solids darkened and became magnetic under heating. In all samples, the Fe(II)/Fe(III) ratios increased with heating; at about 350 °C, they reached values close to the stoichiometric ratio of magnetite (0.5). The curves differed quantitatively in each case, depending on the presence and on the amount of the dopant. Figure 1 illustrates this behavior for samples with Fe/Cu = 35 (with or without chromium), chromium-doped solids and the plain materials. As we can see, at lower temperatures chromium itself does not affect the Fe(III) reduction whereas copper delays this process in the presence or absence of chromium. However, above 300 °C the reduction is favored by copper and, as a synergetic effect of the dopants, this ratio is increased even more. It occurs independently of the amount of copper, as noted by the final values of this ratio, in each case (Table 2).

The residual amount of carbon from the carboxylate decomposition is around 0.5% (Table 2). The carbon content can avoid the addition of graphite, often used as pelletization agent, in commercial formulations of the HTS catalysts¹³. Sodium also remained in the solids after heating in a range of 0.8-4.4%.

X-ray diffractograms, taken after heating at several temperatures, for 2h under nitrogen, did not show any discrete diffraction lines for solids heated to 150 and 200 °C. Heating at 250 °C diffuse lines appear and become more intense as the temperature increases. Figure 2 illustrates this profile for the samples with copper and chromium (Fe/Cu = 35).

At 400 °C, the diffractograms show the pattern of magnetite¹⁶ as we can see in Fig. 3. It can also be noted that both copper and chromium delay crystallization; it is evidenced by a broadening of the diffraction lines as well as by a decrease in their intensities.

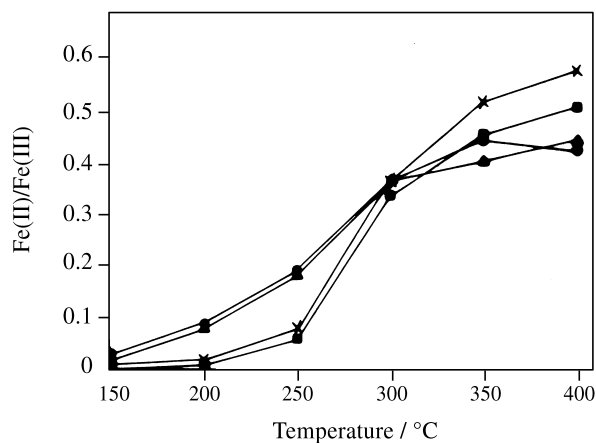
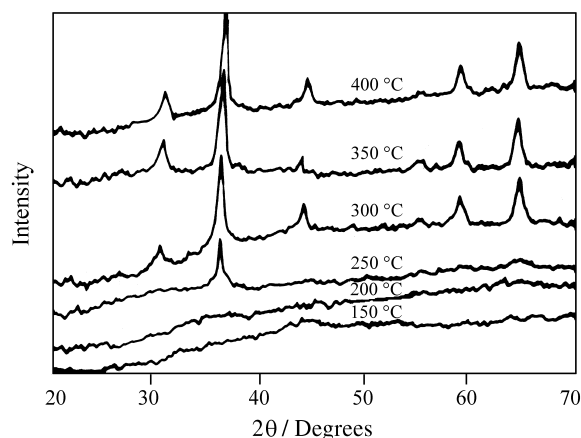


Figure 1. Fe(II)/Fe(III) ratio in plain and doped IHA (Fe/Cu = 35) as a function of the heating temperature • IHA; △ Cr; □ Cu; × CrCu.

Table 2. Fe(II)/Fe(III) molar ratio and the amount of carbon and sodium for plain and doped IHA after heating at 400 °C.

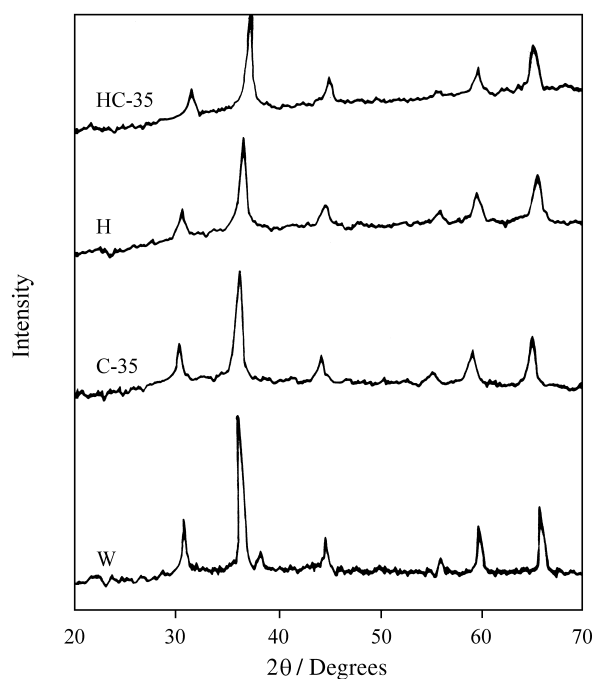
Sample	% Fe (± 0.1)	% Fe(II) (± 0.1)	$\frac{\text{Fe(II)}}{\text{Fe(III)}} \cdot 10$ (± 0.1)	%Cr (± 0.1)	%Cu (± 0.1)	%C (± 0.1)	%Na (± 0.1)
IHA	72.2	21.7	4.3	-	-	0.4	4.4
Cr	60.5	18.8	4.5	14.5	-	0.2	1.1
Cu55	70.3	23.9	4.9	-	1.6	0.6	3.9
Cu35	72.6	24.6	5.1	-	2.6	0.4	1.4
CrCu55	57.0	20.2	5.5	16.0	1.2	0.5	1.0
CrCu35	58.3	21.5	5.8	13.0	1.6	0.6	0.8

**Figure 2.** X-ray diffractograms of Cr- and Cu-doped IHA (Fe/Cu = 35) after heating at several temperatures for 2 h under nitrogen.

From the interplanar spacing values (Table 3) we can note that all dopants enter the magnetite lattice under the experimental conditions used in this work. By comparing the values of the plain samples with those of the ASTM card¹⁶, it is seen that sodium increases the parameters of magnetite, as pointed out earlier¹⁷. In spite of its large radius, this ion can easily enter the spinel structure due to its lower electronegativity (0.9) as compared to that of Fe(II) (1.65) and Fe(III) (1.83); as a result, stronger bonds (Na-O) are produced, as compared to Fe-O ones¹⁸.

On the other hand, chromium leads to a shrinkage of the unit cell due to its smaller radius (0.63 Å) as compared to that of Fe(II) (0.74 Å). It has been accepted that the Cr(III) ion has an octahedral preference due to its stabilization energy in the octahedral field¹⁹ and thus substitutes Fe(II) ion during the spinel formation; as a consequence, the Fe(II) replaced is further oxidized to Fe(III) (0.69 Å) increasing the shrinkage even more.

However, Cu(II) (0.72 Å) does not readily substitute Fe(II) (0.74 Å), in spite of its stabilization energy; this may be attributed to its higher electronegativity leading to Cu-O bonds which are weaker than Fe-O bonds. This had been evidenced by studying natural systems such as silicate

**Figure 3.** X-ray diffractograms of plain and doped IHA (Fe/Cu = 35) previously heated at 400 °C for 2 h under nitrogen.

minerals in which copper does not enter the structure during magmatic crystallization but rather accumulates in the residual magma until a concentration sufficient to precipitate CuFeS_2 is reached¹⁸.

Another phase like chromium oxide was not detected; neither was wustite, despite the high amount of Fe(II) in the solids.

Infrared spectroscopy was used to confirm the presence of acetate in solids, by the detection of the absorption bands at 1530 and 1410 cm^{-1} , assigned to the symmetric and asymmetric stretching modes²⁰ as well as the bands at 3350 and 1330 cm^{-1} due to the hydroxyl and nitrate groups, respectively²¹.

Table 4 shows the surface areas of plain and doped IHA before and after heating under nitrogen at 400 °C for 2 h. All solids have large areas before heating, but they present

Table 3. Interplanar spacings (d) for plain and doped IHA after heating at 400 °C.

hkl	ASTM card N. 19269	d (Å)					
		M	Cr	Cu55	Cu35	CrCu55	CrCu35
220	2.996	3.00	2.95	2.99	2.96	3.00	3.00
311	2.530	2.55	2.51	2.54	2.52	2.53	2.53
222	2.419	2.44	--	2.44	-	-	-
400	2.096	2.11	2.08	2.11	2.09	2.09	2.10
422	1.712	1.72	1.70	1.72	-	1.71	-
333/511	1.614	1.62	1.60	1.62	-	1.61	1.61
440	1.483	1.49	1.47	1.49	-	1.48	1.48

different resistance against sintering. Copper does not act as a textural promoter but rather favors the loss of area; in the presence of chromium, however, this process is delayed. As expected^{1,2,9}, chromium makes magnetite sintering more difficult.

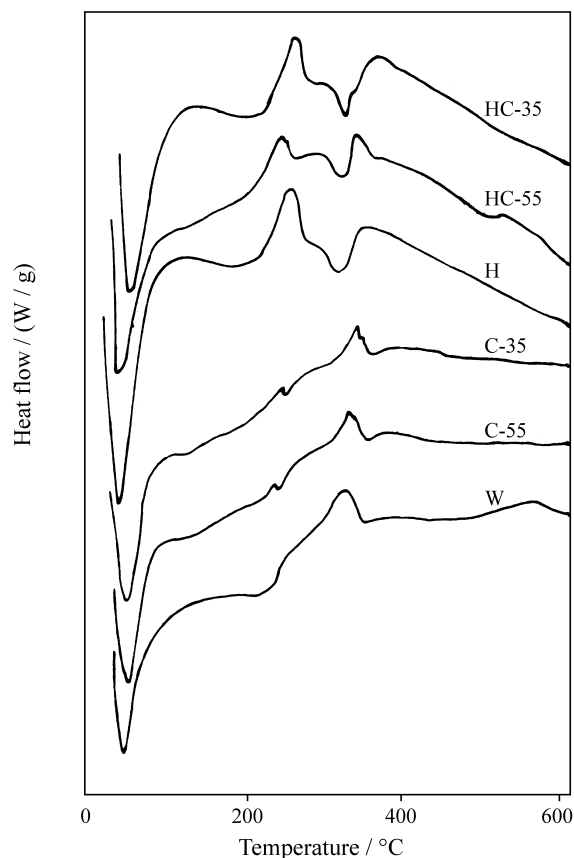
Thermal analysis was performed on IHA samples to monitor the effect of copper on the magnetite formation. However, due to the low amount of this dopant, as well as to the presence of sodium in solids, this effect was not noted. In all cases there was an endothermic peak below 150 °C due to the loss of volatile components^{9,22} and an exothermic one around 320 °C, due to magnetite formation⁹. The thermograms of the chromium-doped IHA show, in addition, an exothermic peak around 244 °C, associated to dehydration²³. An exothermic peak at 450 °C, due to the production of crystalline chromium oxide²⁴, was not detected.

As illustrated in Fig. 4, electron scanning micrographs show coarse particles of variable sizes and shapes, with several fissures and other imperfections. This fact can be attributed to the numerous factors (*e.g.* pH and gradients of concentration) which affect the reactions involved in the ferric hydrous oxides precipitation; in this way, a small change in the preparation conditions may yield different kinds of precipitates²⁵.

From the experiments with the X-ray microprobe it was noted that copper is not distributed evenly on the surface in the 100 µm range and this effect is more intense in chromium-doped solids. In contrast, chromium is more evenly distributed on the surface in all samples. Figure 4 shows a view of chromium and iron distribution; we note that they do overlap in the size of 10-100 µm. By comparing the chemical analysis results with the average values found by X-ray microanalysis (Table 5) we see that most of the chromium is inside the solid. In the same way, copper is distributed non-uniformly along the structure as proposed by Sidhu *et al.*²⁶ In chromium-free samples, it tends to

Table 4. Surface area (m²/g) of plain and doped IHA before and after heating at 400 °C.

Sample	IHA	Cr	Cu55	Cu35	CrCu55	CrCu35
Before	212	223	240	222	198	235
After	20	75	15	13	59	79

**Figure 4.** Scanning electron micrographs taken from Cr- and Cu-doped IHA heated at 400 °C.

migrate to the surface, but in the presence of chromium, it goes from the surface.

Table 5. Fe/Cr and Fe/Cu molar ratio of doped IHA obtained by chemical analysis and by X-ray microanalysis after heating at 400 °C.

Sample	Chemical Analysis		X-ray microprobe (average values)	
	Fe/Cr	Fe/Cu	Fe/Cr	Fe/Cu
Cr	5.3	-	10.1	-
Cu55	-	54.0	-	33.6
Cu35	-	30.2	-	34.0
CrCu55	4.7	45.6	9.7	68.6
CrCu35	3.9	38.9	9.4	41.6

Table 6 presents the results of the catalytic activity towards the HTS reaction as well as the Fe(II)/Fe(III) ratio of fresh and used catalysts.

In agreement with results of several authors¹⁻³ chromium-doped iron oxides are more active than the plain solids and this is due to the action of chromium as textural promoter. In fact, we found that the activity per unit area of chromium-doped magnetite is lower than that of the pure iron oxide. In contrast, copper favors sintering as shown in Table 4. Because of this, the copper-doped solids show activities close to that of the plain catalyst, in spite of their higher activities per unit area. In doped-samples with both chromium and copper, there is a better performance only in solids with greater amounts of copper (Fe/Cu = 35), since chromium tends to cause a decrease in the activity per unit area. As magnetite is the active phase we can consider that the activity per unit area is closely related to the intrinsic activity. We can thus conclude that copper acts as a structural promoter in iron-based catalysts whereas chromium leads to a decrease in the intrinsic activity. The chromium-doped magnetite with Fe/Cu = 35 showed a better performance than a commercial catalyst based on copper and chromium-doped hematite ($25.0 \times 10^{-3} \text{ mol g}^{-1} \text{ h}^{-1}$).

From the values of the Fe(II)/Fe(III) ratio of fresh and used catalysts it can be noted that magnetite underwent further reduction in the atmosphere of the HTS reaction, reaching values higher than the stoichiometric value of magnetite. However, it seems that the performance of the catalysts is not altered.

Discussion

It is well-known²⁷⁻³² that Fe(III) and Cr(III) ions exhibit very different behaviors towards hydrolysis and condensation in aqueous solutions, despite their similar electronegativities and coordination numbers. Both form octahedral complexes, but Fe(III) produces very reactive polycations³¹ while Cr(III) leads to stable ones³². This can be correlated with the high rate of condensation of the aquo-hydroxo precursors of Fe(III) ions in contrast with Cr(III) ions. Due to the $3d^3$ electronic configuration, both olation and oxola-

Table 6. Catalytic activity (a), catalytic activity per area(a*) and Fe(II)/Fe(III) ratio of plain and doped magnetite.

Sample	a $\times 10^3$ ($\text{mol g}^{-1} \text{ h}^{-1}$)	Fe(II)/Fe(III) $\times 10$ (± 0.1)		a* $\times 10^4$ ($\text{mol m}^{-2} \text{ h}^{-1}$)
		Fresh catalyst	Used catalyst	
M	8.4	4.3	5.5	4.2
Cr	17.5	4.5	7.1	2.3
Cu55	9.7	4.9	8.2	6.5
Cu35	11.7	5.1	9.1	9.0
CrCu55	19.4	5.5	8.8	3.3
CrCu35	29.8	5.8	11.1	3.8

tion are rather slow processes for Cr(III) which allowed a detailed study as a function of pH³³; this is related to its high crystal field stabilization in the octahedral symmetry. The most crystal field-stabilized ion would be the least hydrolyzed since OH^- presumably produces a weaker field than H_2O . In contrast, olation reaction rates must be decreased as the crystal field stabilization increases, since it implies a decrease of the reactivity of the cation towards the ligand exchange. In fact, chromium complexes are known to be strongly inert²⁸ with several chemical species in slow equilibrium formed simultaneously as the pH increases. On the other hand, Fe(III) cation ($3d^5$) exhibits no crystal field stabilization in the same symmetry and thus the rates of hydrolysis and polymerization are higher than those of the Cr(III) ions. As a consequence, Cr(III) ions produce amorphous gels whose compositions range from $\text{Cr}(\text{OH})_3(\text{OH}_2)_3$ to Cr_2O_3 ^{28,33} while Fe(III) ions form gelatinous precipitates. Their compositions are intermediate between α - FeOOH (goethite) and α - Fe_2O_3 (hematite)^{34,35}.

As far as the divalent transition metal ions are concerned, compact tetramers are formed as a result of the condensation²⁸. However, Cu(II) seems to produce $[\text{Cu}(\text{OH})_2]_\infty$ edge-sharing chain³⁶ due to Jahn-Teller effect typical of d^9 ions in octahedral field. At low pH, a corner-sharing dimer $[\text{Cu}_2(\text{OH})(\text{OH}_2)_2]^{3+}$ is probably formed³⁷ which transforms itself into edge-sharing chain polymers $[\text{Cu}_n(\text{OH})_{2n-2}(\text{OH}_2)_2]^{2+}$ ($n = 2,3$) at higher pH^{37,38}.

In all cases, the kinetics of polymerization in an aqueous medium strongly depend on the charge, size, electronegativity and electronic configuration of the metallic ion^{39,40}: the smaller the charge and the larger the ionic radius the faster will be the process. As a consequence, the dimerization rate constant of the Fe(III) precursor is rather low ($k = 10^{-1} - 10^{-3} \text{ M}^{-1} \text{ s}^{-1}$) whereas it is much faster for Cu(II), $k = 10^8 \text{ M}^{-1} \text{ s}^{-1}$ ^{41,42}.

By considering these aspects, one can suppose that under the experimental conditions used in this work, Fe(III) undergoes hydrolysis and further polymerization simulta-

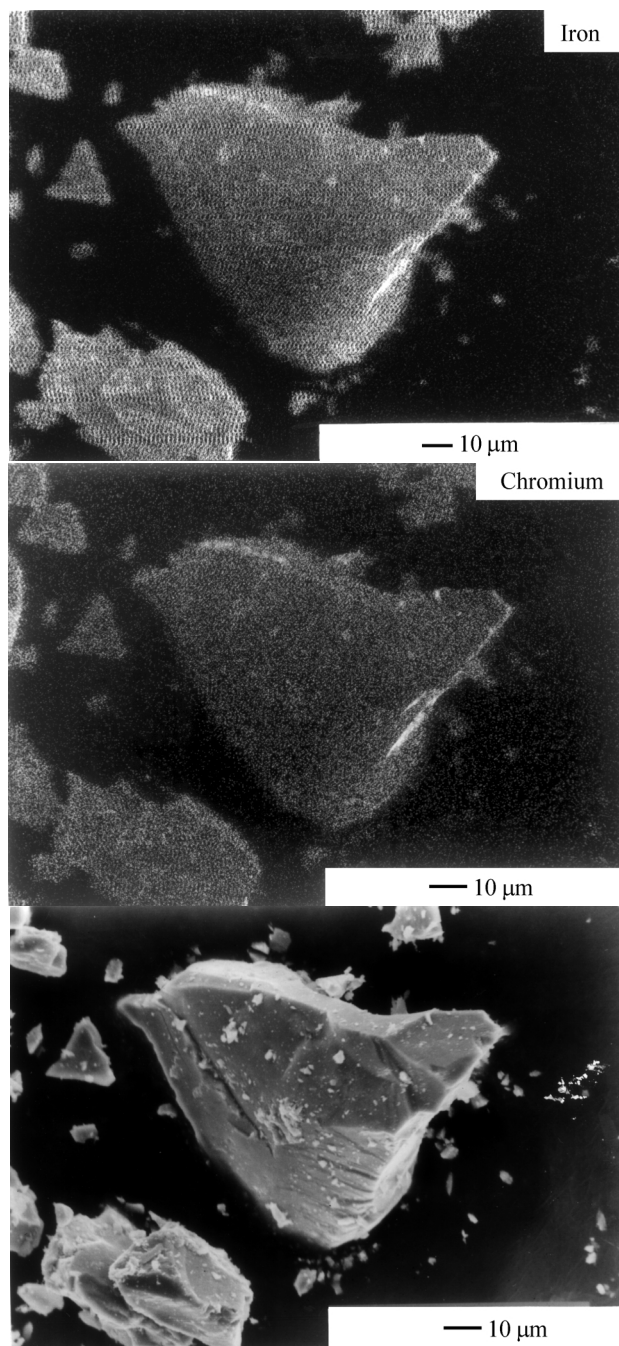


Figure 5.

neously with Cr(III) and Cu(II) ions producing mixed chain polymers. After rinsing with an ammonium acetate solution, this gel is transformed into iron(III)hydroxoacetate (IHA), with acetate ions presumably linked to metal ions⁹. As the Cr(III) ions will form more stable complexes, they will make the iron chains more inert while Cu(II) will do the opposite. Therefore, a chromium-doped IHA chain will be more inert than a plain IHA one; the reverse would be expected for the copper-doped samples.

Under heating the plain and doped-IHA produce magnetite. As reported previously⁹, in chromium-doped samples the species are hampered to react, to sinter or to crystallize because their compounds are inert. Consequently, these solids are less crystalline and have higher surface areas as compared to the plain materials. On the other hand, in copper-doped samples, the species have higher mobilities and the resulting solids are more crystalline and have lower surface areas than pure magnetite; these effects increase with the amount of copper. However, due to the small amounts of this metal in the sample studied a significant effect was noted only in surface areas.

By comparing the chemical analysis results (Table 2) with our previous work⁹ (in which we typically found values of the Fe(II) to Fe(III) molar ratio close to 0.5, in chromium-doped magnetite) we note that the preparation method as well as the presence of Na(I) ions slightly delays Fe(III) reduction probably due to the stronger Na-O bonds¹⁸. In addition, the effect of chromium in the inhibition of the Fe(III) reduction was not found in the present work; as pointed out earlier⁹, the extent of this process strongly depends on the preparation method of the solids. However, the presence of chromium leads to a decrease in the amount of sodium, suggesting a preference of the spinel structure in accepting Cr(III) instead of Na(I) ions. Such behavior can be explained by the Goldschmidt Rules¹⁸, according to which the ion with the smaller radius or the higher charge will be preferentially incorporated.

In the same way, the surface areas of the plain magnetite are lower than those prepared earlier ($33 \text{ m}^2/\text{g}$)⁹; again, this fact can be attributed to the differences in the preparation methods which reflect different particles size⁴³.

No other phase, besides magnetite, was detected. As wustite is unstable below $575 \text{ }^\circ\text{C}$ ⁴⁴, it is not probable that this phase could be in the solids produced in the present work. By studying the reduction of iron oxides, it has been noted⁴⁵ that metallic iron is formed directly from magnetite below that temperature, but through the intermediate wustite phase above $575 \text{ }^\circ\text{C}$. In addition, according to several authors^{46,47} the lattices of iron catalysts promoted with oxides of trivalent cations of metals are paracrystalline due to endotactic groups $\text{X}_2\text{Fe}_2\text{O}_4$ (X = trivalent cation) which are statistically distributed in the structure. This can explain the excess of Fe(II) in doped-solids, as compared to our previous work, and the differences detected in the interplanar spacing values.

Both chromium and copper improve the performance of the catalysts. Chromium acts as a stabilizer but leads to a decrease in the intrinsic activity, in contrast with other works^{48,49} in which the specific activity and activation energy of the iron-based catalysts appear to be about the same with or without Cr_2O_3 addition. This can be attributed to the different phases present in each case. As pointed out by Sengupta *et al.*⁵⁰, the intrinsic activity as well as the

stability of the catalysts depends on the phases present in the solids. In fact, a Cr₂O₃ phase was not detected in this work.

On the other hand, copper improves the intrinsic activity and this effect depends on the amount of this dopant in the solids; the highest value is shown by the sample with Fe/Cu = 35. In the presence of chromium there is a decrease, leading to values near those of the plain magnetite. However, as chromium delays sintering, chromium and copper improve the catalytic performance as a synergetic effect of these dopants.

Conclusions

Copper improves the performance of the iron and chromium-based catalysts towards the HTS reaction, by increasing the intrinsic activity. This effect increases with the amount of this dopant in solids. It favors sintering leading to solids with low surface areas but in the presence of chromium sintering is delayed and this results in catalysts with higher activity.

Acknowledgement

The authors are grateful to Professor Fernando Galembeck for his help in characterizing the catalysts. EBQ acknowledges CNPq for an undergraduate fellowship. The work was performed under the financial support of CNPq and FINEP.

References

- Campbell, J.S.; Young, P.W. In *Catalysis Handbook*; Wolfe Scientific Books; London, 1970.
- Newsome, D.S. *Catal. Rev.- Sci. Eng.* **1980**, *21*, 275.
- Bohlbro, H. In *An Investigation on the Kinetics of the Conversions of Carbon Monoxide with Water Vapor over Iron Oxide based Catalysts*; The Haldor Topsoe Laboratory, Vedback, 1960.
- Andreev, A.; Idakiev, V.; Kostov, K.; Gabrovska, M. *Catal. Lett.* **1995**, *31*, 245.
- Li, Y.; Wang, R.; Zhang, J.; Cahng, L. *Catalysis Today* **1996**, *30*, 49.
- Xue, E.; O'Keefe, M.; Ross, J.R.H. *Catalysis Today* **1996**, *30*, 107.
- Souza, M.O.G.; Quadro, E.B.; Rangel, M.C. *Química Nova* **1998**, *21*, 428.
- Idakiév, D. *React. Kinet. Catal. Lett.* **1988**, *33*, 119.
- Rangel, M.C.; Sasaki, R.M.; Galembeck, F. *Catal. Lett.* **1995**, *33*, 237.
- Abreu Filho, P.P.; Pinheiro, E.A.; Galembeck, F. *Reactivity of Solids*. **1987**, *3*, 241.
- Fergl, F.; Anger, V.; Oesper, R.E. *Inorganic Analysis*; Elsevier, Amsterdam, 1972.
- Vogel, A.I. *Quantitative Inorganic Analysis*, Longman, London, 1961.
- Bennet, H.; Reed, R.A. *Chemical Methods of Silicate Analysis. A Handbook*. Academic Press, London, 1971.
- Basolo, F.; Johnson, R. *Química de los Compuestos de la Coordinación*; Editorial Reverté, S.A., Barcelona, 1980.
- Styles, A. *Catalyst Manufacture. Laboratory and Commercial Preparations*; Marcel Dekker, Inc. New York, 1983.
- ASTM card no. 19 269.
- Dry, M.E.; Ferreira, L.C. *J. Catal.* **1967**, *7*, 352.
- Ringwood, A.E. *Geochimica et Cosmochimica Acta* **1955**, *7*, 189.
- McClure, D.S. *J. Phys. Chem. Solids* **1957**, *3*, 311.
- Silverstein, R.; Basslerand, G.C.; Morrill, T.C. *Spectrometry Identification of Organic Compounds*; John Wiley and Sons, New York.
- Niquist, R.A.; Kagel, R.O. *Infrared Spectra of Inorganic Compounds*, Academic Press Inc.; Orland, 1971.
- Rangel, M.C.; Galembeck, F. *J. Catal.* **1994**, *145*, 364.
- Pascal, P. *Nouveau Traité de Chimie Minérale. Tome XVII.*; Masson et Cie, Paris, 1967.
- Bhattacharga, S.K.; Ramachandram, V.S.; Ghosh, J.C. *Advances in Catalysis* **1957**, *9*, 114.
- Matijevic, E.; Scheiner, P. *J. Colloid Interf. Sci.* **1978**, *63*, 509.
- Sidhu, P.S.; Gilkes, R.J.; Posner, A.M. *J. Inorg.Nucl. Chem.* **1978**, *40*, 429.
- Baes Jr., C.F.; Mesmer, R.E. *The Hydrolysis of Cations*. John Wiley and Sons, New York, 1976.
- Livage, J.; Henry, M.; Sanchez, C. *Progr. Sol. State Chem.* **1988**, *8*, 259.
- Burguess, J. *Metal Ions in Solution*; John Wiley and Sons, New York, 1978.
- Blesa, M.A.; Matijetic, E. *Adv. Colloid Interf. Sci.* **1989**, *29*, 173.
- Segal, D.L. *J. Chem.Tech. Biotechnol.* **1984**, *24*, 355.
- Khoe, G.H.; Brown, P.L.; Sylva, R.N.; Robins, R.G. *J. Chem. Soc. Dalton Trans.* **1986**, 1901.
- Stunzi, H.; Spiccia, L.; Rotzinger, F.P.; Marty., W. *Inorg.Chem.* **1988**, *28*, 66.
- Rajendram, S.; Rao, Y.S.; Maiti, H.S. *J.Mater. Sci.* **1982**, *19*, 2709.
- Prasad, S.V.S.; Rao, V.S. *J. Mater. Sci.* **1984**, *19*, 3266.
- Perrin, D.D. *J. Chem. Soc.* **1960**, 3189.
- Sylva; R.N.; Davidson, M.R. *J. Chem. Soc. Dalton Trans.* **1979**, 232.
- Eigen, M. *Pure Appl. Chem.* **1963**, *69*, 97.

39. Kruger, H. *Chem. Soc. Rev.* **1982**, *11*, 227.
40. Lutz, B.; Wendt, H. *Chimia*, **1973**, *27*, 575.
41. Wendt, H. *Chimia* **1973**, *27*, 575.
42. Viswanath, R.P.; Viswanath, B.; Sastri, M.V.C. *Thermochim. Acta* **1976**, *16*, 240.
43. Matijevic, E.; Sapieszco, R.S.; Melville, J.B. *J. Colloid Interf. Sci.* **1975**, *50*, 567.
44. Graham, M.J.; Channing, D.A.; Swallow, G.A.; Jones, R.D. *J. Mat. Sci.* **1975**, *10*, 1175.
45. Ray, H.S.; Kundu, N. *Thermochim. Acta* **1986**, *101*, 107.
46. Hosemann, R.; Preisinger, A.; Vogel, W. *Ber. Bunsenges. Phys. Chem.* **1966**, *70*, 796.
47. Ludwiczek, H.; Preisinger, A.; Fischer, A.; Hosemann, R.; Schonfeld, A.; Vogel, W. *J. Catal.* **1978**, *51*, 326.
48. Markina, M.I.; Bareskov, G.K.; Ivanovskii, F.P.; Lyndkovskaya, B.J. *Kinet. Katal.* **1961**, *2*, 867.
49. Danielczyk, N.; Haber, J. *Rocz. Chem.* **1977**, *51*, 507.
50. Sengupta, G.; Prasad, K.; Sinha, S.C.; Sem, S.P. *Indian J. Chem.* **1979**, *18*, 392.

Received: November 27, 1997